ELSEVIER

Chemical Engineering Journal 136 (2008) 306–311

Chemical Engineering Journal

www.elsevier.com/locate/cej

Drop dispenser in a cross-junction microfluidic device: Scaling and mechanism of break-up

J. Tan, J.H. Xu, S.W. Li, G.S. Luo *

The State Key Lab of Chemical Engineering, Department of Chemical Engineering, Tsinghua University, Beijing 100084, China

Received 24 January 2007; received in revised form 14 March 2007; accepted 3 April 2007

Abstract

This paper presents a new symmetrical flow route of perpendicular rupturing to realize the controllable preparation of monodisperse O/W and W/O emulsions by using a cross-junction microfluidic device. Uniform plugs ranging from 300 to 1800 μm were successfully prepared. The effect of surfactants on two-phase flow performance, two-phase flow patterns under different continuous phase and dispersed phase flow, and the influences of flow rates and the viscosity of continuous phase on plug length were studied. The formation mechanisms of plug flow have been discussed. Considering both the equilibrium between shear force of the continuous flow and interfacial tension, the wetting property between dispersed phase and walls of microchannel, and the influence of oil/water flow ratio on the shape of the interface, a quantitative equation was developed to predict the plug length, which is consistent with the experimental results.

Keywords: Microfluidic; Symmetrical; Monodisperse; Emulsion

1. Introduction

Emulsions have gained a great of attention for their wide applications in the textile industry, medicament, food, chemical industry, and so on. Emulsions are commonly divided into oil-in-water (O/W) and water-in-oil (W/O). For the thermodynamical metastability of emulsions, a surfactant is commonly introduced into the systems to stabilize the droplet against coalescence. Precise control of droplet size and polydispersity is demanded in many important potential applications of emulsions. Some tactics have been performed to reduce the polydispersity of droplets [1,2]. In the recent years, droplet-based applications has expanded from conventional systems to microanalysis, protein crystallization, and on-chip separation because of the development of micromaching techniques [3–5]. Monodispersed droplets in microfluidic devices have been prepared through many methods, including geometry-dominated break-up [6–8], crossflow rupturing through microchannel arrays [9], hydrodynamic flow focusing through a small orifice [10–12], and two-phase crossflowing rupture streams in T-junction microchannels [3,4,13–15]. Highly uniform emulsion droplets with polydispersity indexes less than 5% could be prepared [6–8,13]. In microfluidic devices, W/O emulsions were prepared in hydrophobic microchannels [8,10,13,15–17] and O/W emulsions in hydrophilic microchannels [9,11,18–20].

In our previous work, a new flow route, which is so-called perpendicular shear force induced break-up, was developed to prepare monodisperse droplet in a T-junction microfluidic device using a quartzose capillary embedded into the perpendicular channel as the water-phase flow channel [21]. Ordered flow of oil drops could be formed when the contact angle between oil phase and microchannel wall is more than 90. Controllable preparation of monodisperse W/O and O/W emulsions in the simple T-junction microfluidic device could be achieved by changing the wetting properties of the microchannel walls with different surfactants [22].

Based on our previous work, we are trying to further understand the fundamentals of the microchannel dispersion process and prepare emulsions more controllable. Monodisperse microbubbles formation in a similar cross-junction microfluidic device has been reported [23], while the droplet formation mechanism in cross-junction microfluidic device has not been reported yet. In this work, we developed a symmetrically perpendicular rupturing technique to realize the dispersion of liquid–liquid

* Corresponding author. Tel.: +86 10 62783870; fax: +86 10 62783870.
E-mail address: gsluo@tsinghua.edu.cn (G.S. Luo).

1385-8947/$ – see front matter © 2007 Elsevier B.V. All rights reserved.
doi:10.1016/j.cej.2007.04.011

systems in a cross-junction microdevice. In the cross-junction microfluidic device, no quartzose capillary was embedded but two perpendicular channels were instead. The controllable preparation of both W/O and O/W emulsions in the same microchannel was realized by changing the wetting properties of the wall. Two-phase flow patterns were dependent on the flow rates of continuous phase and dispersed phase. The effects of surfactants, two-phase flow rates, and continuous viscosity on dispersed phase plug length have been investigated. A discussion about the equilibrium between shear force of the continuous flow and interfacial tension, the wetting property between dispersed phase and microchannel wall, and the influence of oil/water flow rate on the shape of the interface has been made. Comparison of different methods could be easily made and the influence of different forces on the liquid–liquid dispersion process could be found. Finally, the droplet formation mechanisms of plug flow have been discussed, and a quantitative equation was utilized to predict the plug length accurately whose results may induce to develop new techniques and new models.

2. Experimental

2.1. Microfluidic device

A cross-junction microfluidic device was used, which was fabricated on a 100 mm × 20 mm × 5 mm polymethyl methacrylate (PMMA) plate using an end mill. The straight channel dimension is approximately 250 μm wide × 200 μm high, and the perpendicular ones dimensions are 150 μm wide × 100 μm high (Fig. 1). The microfluidic device was sealed using another PMMA thin plate with 1 mm thickness by curing at 105 °C using high pressure thermal sealing techniques. Three microsyringe pumps were used to pump the two phases into the two-phase flow channels, respectively.

2.2. Materials

Anhydrous octane, hexadecane were used as the oil phase, respectively. Deionized water, aqueous solutions with 24 wt.%, 52 wt.%, and 62 wt.% glycerol were used as the water phase, respectively. Different concentrations of Span 80 used as the oil-soluble surfactants were added to the oil phase. Different concentrations of Tween 20 used as the water-soluble surfactants were added into the water phase. The surfactant concentration is ranged from 0.5 to 3.0 wt.%.

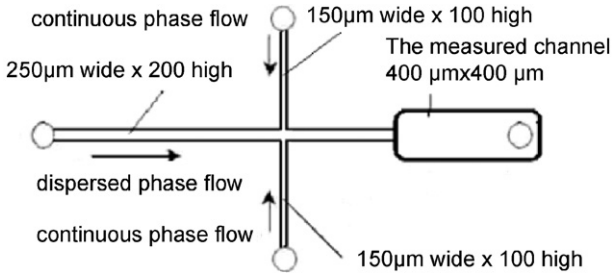

Fig. 1. The cross-junction microfluidic device.

2.3. Apparatus and analysis

The interfacial tension was measured by an interfacial tension meter using the spinning drop technique (XZD-3, China). Droplet formation experiments were carried out with a microscope at the magnification of 100×. A highspeed CCD video camera was connected to the microscope, and the images were recorded at a frequency of 200 images/s. The lengths of the plugs were measured from microscope images. After changing any of the flow parameters, we allowed at least 100 s of equilibration time.

3. Results and discussion

3.1. Effect of surfactants on two-phase flow performance

In our previous study, the wetting properties between the fluids and the wall surfaces deserved particular emphasis of two-phase flow in microchannels [22]. Ordered flow of drops could be formed when the contact angle between dispersed phase and microchannel wall is more than 90. The critical micelle concentration (C_{mc}) of Span 80 in octane is close to 0.03 wt.%, when the concentration ranges from 10^{-4} to 0.03 wt.%, the interfacial tension decreases from 58.0 to 3.2 mN/m, and the interfacial tension retains the minimum value at higher concentrations. On the other

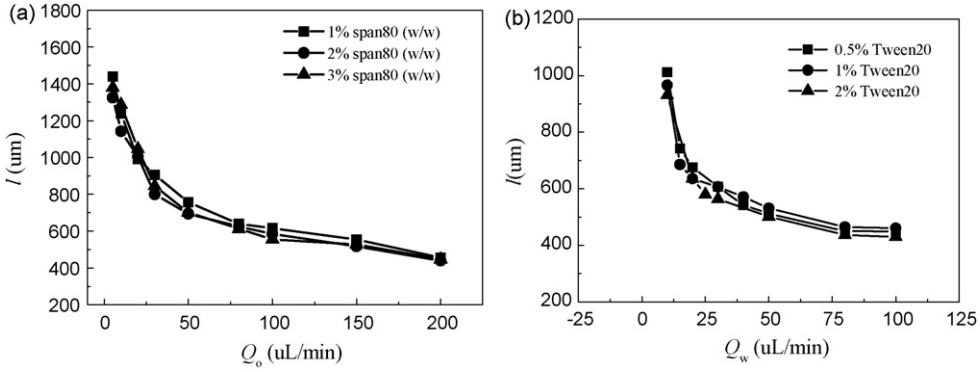

Fig. 2. Effect of surfactant concentration on the plug length: (a) W/O system with Span 80 as surfactant in oil phase, Q_w = 5 μm/min; (b) O/W system with Tween 20 as surfactant in water phase, Q_o = 5 μm/min.

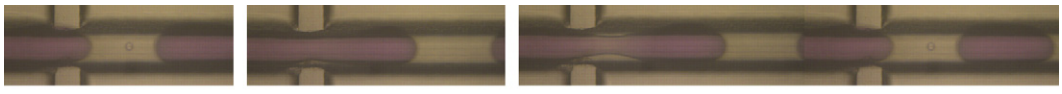

Fig. 3. Evolution of the oil–water interface with Span 80 as surfactant in oil phase and at surfactant concentration of 2.0 wt.%. Water phase flow rate was 5 μL/min and oil phase flow rate 10 μL/min: (a) $t = 0$ s; (b) $t = 0.04$ s; (c) $t = 0.08$ s; (d) $t = 0.12$ s.

hand, the C_{mc} of Tween 20 in water is close to 0.1 wt.%, when the concentration ranges from 10^{-4} to 0.1 wt.%, the interfacial tension decreases from 58.0 to 4.8 mN/m, and the interfacial tension retains the minimum value at higher concentrations [22].

We examined the effects of surfactants and their concentrations on the two-phase flow properties with different experimental systems. Ordered water-dispersed flow regimes appears when Span 80 added into oil phase, the concentration of which is higher than 0.03 wt.%. Ordered oil-dispersed flow regimes appears when Tween 20 added into oil phase, the concentration of which is higher than 0.1 wt.%. So ordered water-dispersed and oil-dispersed flow regimes could be achieved, which is similar to that of previous work [22]. Fig. 2a and b shows the effect of the surfactant concentration on the length of dispersed phase plugs when its concentration is higher than the C_{mc}. The droplet diameter was independent of surfactant concentration mainly because that the interfacial tension reaches the minimum value when the surfactant concentration is more than C_{mc}.

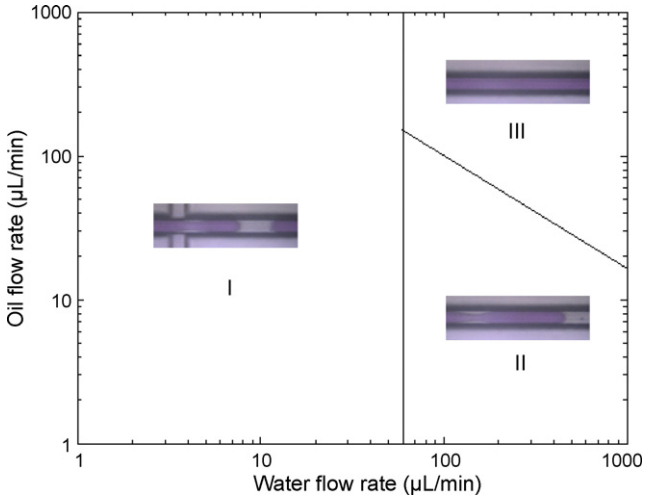

Fig. 4. Flow patterns with different two-phase flow rates. Continuous phase (oil phase) was 2.0 wt.% Span 80 *n*-octane solution and dispersed phase (water phase) was deionized water: (I) water plugs broke at the junction of the microchannel; (II) water plugs broke after a period of laminar flow; (III) two phases keep laminar flow in the microchannel.

3.2. Two-phase flow patterns

We imaged the intersection and observed the evolution of the water–oil interface shape. From the recorded images, a single plug break-up process could be described into three stages (Fig. 3). Firstly the water thread penetrates into the outlet channel (Fig. 3b). Secondly, the vertical oil flow causes the development of a clear water thread neck and the width decreases at a certain rate (Fig. 3c). In the third stage, the water thread collapses and breaks up rapidly, retracts upstream in the outlet channel, and the whole process starts again (Fig. 3d).

Furthermore, different two-phase flow patterns were obtained depending on the changing of continuous phase and dispersed phase flow rates. Fig. 4 shows the situation of different flow patterns obtained using octane as the continuous phase and water as the dispersed phase. At low dispersed phase rates, the shear force from the continuous phase is high enough to induce the dispersed phase to disperse into plugs at the junction of the microchannel. When we increase the dispersed phase rate at low continuous phase rates, the shear force from the continuous phase is not high enough to induce the dispersed phase to disperse into plugs at the junction of the microchannel, in this case, plugs could be formed after an uncertain distance laminar flow. When we increase the continuous phase rate at high dispersed phase rates, the distance of laminar flow could increase until the formation of plugs is not observed in the microchannel. We keep

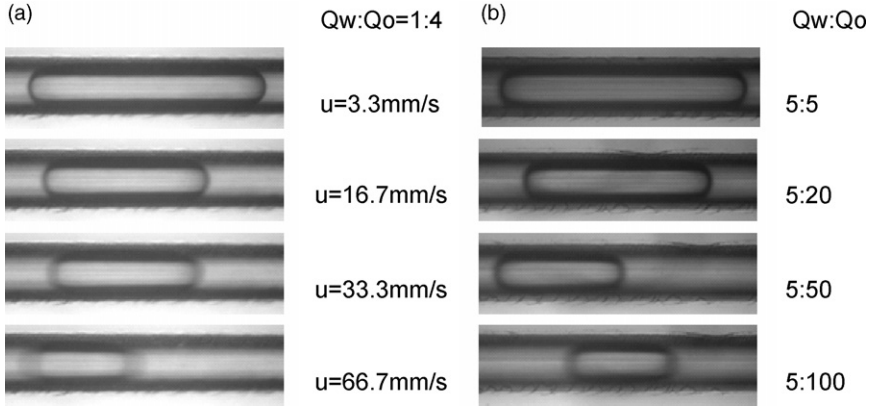

Fig. 5. Micrographs illustrating the influences of two-phase rates on water plugs: (a) total flow velocity and (b) oil flow rate.

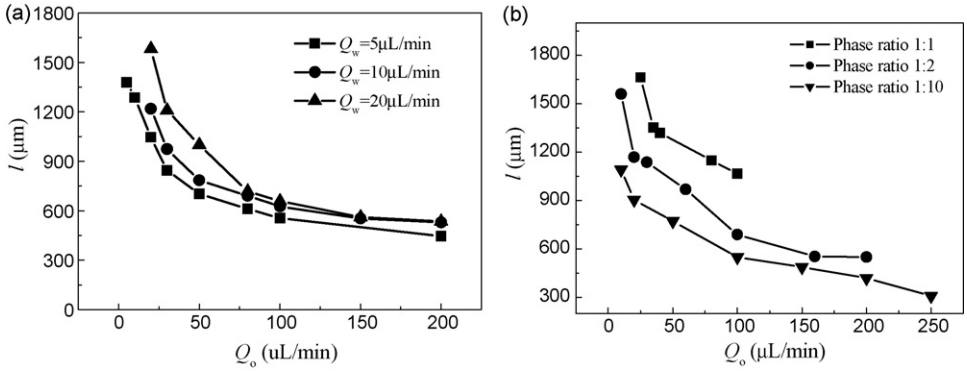

Fig. 6. Influences of two-phase flow rates on water plug length: (a) total flow rate and (b) ratio of oil and water flow rate.

the two-phase flow patterns as the first regime above to assure the repeatability of the experiment.

3.3. Effect of flow rates on plug length

Fig. 5a and b shows the micrographs of dispersed phase plugs under different total flow rates at a constant value of Q_c/Q_d, where Q_c is the flow rate of the continue phase, Q_d is the flow rate of the dispersed phase, Q_w is the flow rate of the water phase and Q_o is the flow rate of the oil phase, and under different continuous phase flow rates with a fixed dispersed phase rate of 5 μL/min, which used octane as the continuous phase and water as the dispersed phase. Fig. 6a and b shows the effects of the value of total flow rate and Q_c/Q_d on dispersed phase plug length in W/O system, and the ones in O/W system are shown as Fig. 7a and b. As shown in these figures, the dispersed phase plug length decreases as continuous phase flow rate increasing at a fixed dispersed phase rate, and also decreases as total flow rate increasing at a constant value of Q_c/Q_d.

3.4. Effect of the viscosity of continuous phase on plug length

We used hexadecane as the continuous phase comparing with octane in W/O system, and used aqueous solution with 24, 52, 62 wt.% as the continuous phase comparing with water in O/W system, to decide the effect of the viscosity of continuous phase on plug length. As shown in Fig. 8a and b, in which l means the plug length and μ means the viscosity of continuous phase, the dispersed phase plug length decreases with the increase of continuous phase viscosity.

3.5. Discussion of plug formation mechanisms

The plug length decreased with the increase of continuous phase and total flow rates, and the viscosity of the continuous phase, while increased slightly with the increase of dispersed phase flow rate. These results are different from the one in our previous work which used the asymmetrically perpendicular rupturing in the T-junction microfluidic [21], in which the pug length decreased with increasing Q_w/Q_o, while independent of the total flow rate and the viscosity of continuous phase. The difference may attribute to the symmetrical flow route. In asymmetrical flow route of perpendicular rupturing, the main effect on plug sizes is the change of water–oil interface shape during collapse, which is dependent on two-phase flow rate and contact angle between oil and the microchannel wall for a given working system. While in the case of symmetrical flow route of perpendicular rupturing, the wall was replaced by another water–oil interface at the junction. And the effect of channel wall was weakened, while the effect of continuous phase shear force increased and played an important role during droplet breakup.

On the other hand, in the case of bubble formation using symmetrical flow route, the slug length was also independent of the total flow rate and the viscosity of continuous phase. The differ-

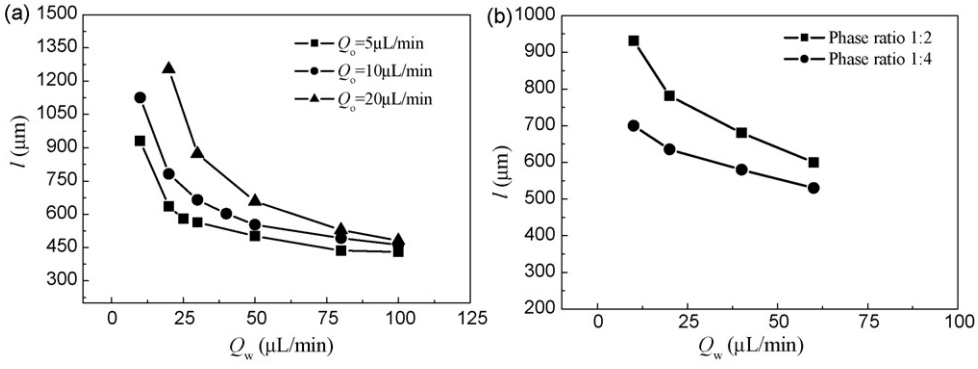

Fig. 7. Influences of two-phase flow rates on oil plug length: (a) total flow rate and (b) ratio of water and oil flow rate.

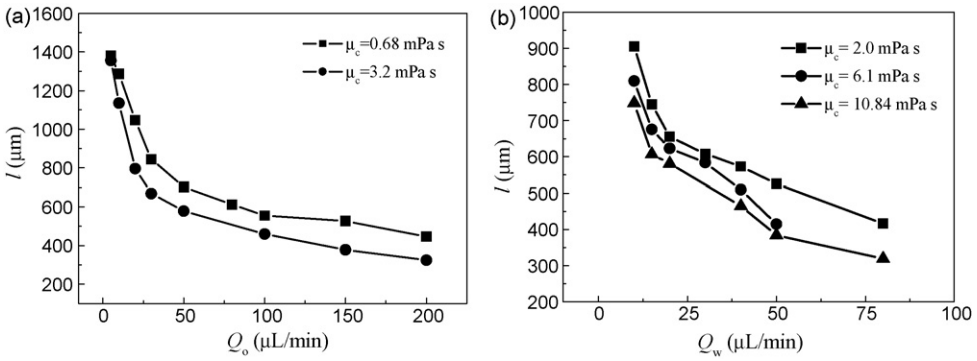

Fig. 8. Influence of continuous phase viscosity on plug length: (a) W/O system and (b) O/W system.

ence between bubble and plug formation might be the variety of values of capillary number ($Ca = \mu u/\gamma$, where μ is the viscosity, u is the velocity of the carrier fluid, and γ is the interfacial tension). In bubble formation process, the interfacial tension between water and air was about 73 mN/m, and the interfacial tension between air and the mixture of water and sodium dodecyl sulfate (SDS) was about 38 mN/m [23]. While in plug formation, the interfacial tension between water phase and oil phase was about 2 mN/m. The capillary numbers in bubble formation were typically small ($Ca < 10^{-2}$), which was at the magnitude of 10^{-2} in plug formation process. As previous experimental results and numerical simulations, there is a critical value of the capillary number ($Ca_{CR} \sim 10^{-2}$) above which the shear stresses start to play an important role in the process of break-up [24,25]. This might explain the influence of the total flow rate and the viscosity of continuous phase on the plug length in our experiments.

Considering the two types of influences on the plug length, one is wetting property and the shape of the interface, which could be effected by the ratio of the continuous phase and the dispersed phase Q_c/Q_d mostly; the other is the equilibrium between shear force of the continuous flow and interfacial tension, which could be effected by capillary number Ca mostly. We assume the plug length could be correlated as

$$\frac{l}{w} = k\left(\frac{Q_c}{Q_d}\right)^{\alpha} Ca^{\beta} \tag{1}$$

Linear regression was used to evaluate the data got in the experiments. The resulted equation is

$$\frac{l}{w} = 1.59\left(\frac{Q_c}{Q_d}\right)^{-0.20} Ca^{-0.20} \tag{2}$$

where l is the dispersed phase plug length, w is the width of the microchannel, Q_c is the continuous phase flow rate, Q_d is the dispersed phase flow rate, and Ca is the capillary number. Although this model is relatively simple with only three empirically derived constants, it appears to provide a good fit across the whole range of data, as shown in Fig. 9.

It is therefore useful in predicting the dispersed phase plug length in the microfluidic device.

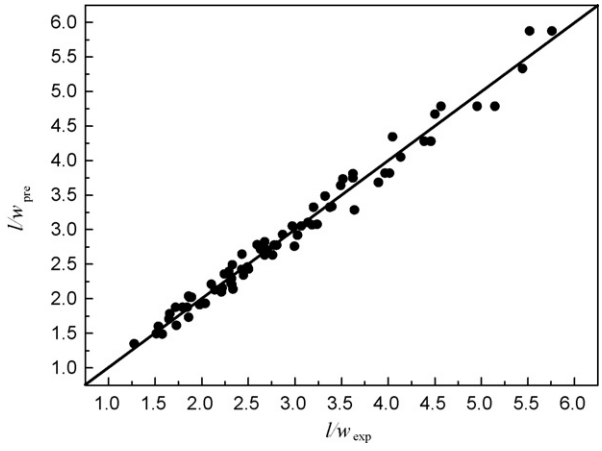

Fig. 9. Comparison between correlated values and experimental data. The correlated value was calculated using Eq. (2).

4. Conclusions

We have presented a new symmetrical flow route of perpendicular rupturing to realize the controllable preparation of monodisperse O/W and W/O emulsions by using a cross-junction microfluidic device. Wetting properties of the fluids to the walls determined the two-phase flow conditions. We could prepare W/O and O/W emulsions by adding different surfactant into oil or water phase to changing the contact angle between fluids and channel wall. The two-phase flow patterns are dependent on the flow rates of continuous phase and dispersed phase. The dispersed phase plug decreased with the increase of continuous phase and total flow rates, as well as the viscosity of the continuous phase, while increased slightly with the increase of dispersed phase flow rate. The formation mechanisms of plug flow have been discussed. Comparing with plug formation mechanisms with asymmetrically perpendicular rupturing in T-junction microfluidic device, the effect of wetting property is weakened, the shear force increases, and the value of Ca is above the critical value. As a result, the shear stresses play an important role in the process of break-up. Considering the equilibrium between shear force of the continuous flow and interfacial tension, the wetting property between dispersed phase and microchannel wall, and the influence of oil/water flow rate on the shape of the interface, a empirical equation was

developed to predict the plug length accurately. The empirical equation will be useful for the precise controllable preparation of monodisperse emulsions.

Acknowledgments

We would like to acknowledge the Department of Biological Sciences and Biotechnology at Tsinghua University for providing the microfluidic device. We also gratefully acknowledge the support of the National Natural Science Foundation of China (20476050, 20490200, and 20525622) and SRFDP (20040003032) for this work.

References

[1] T.G. Mason, J. Bibette, Shear rupturing of droplets in complex fluids, Langmuir 13 (1997) 4600–4613.
[2] P.B. Umbanhowar, D.A. Weitz, Monodisperse emulsion generation via drop break off in a coflowing stream, Langmuir 16 (2000) 347–351.
[3] H. Song, R.F. Ismagilov, Millisecond kinetics on a microfluidic chip using nanoliters of reagents, J. Am. Chem. Soc. 125 (2003) 14613–14619.
[4] B. Zheng, L.S. Roach, R.F. Ismagilov, Screening of protein crystallization conditions on a microfluidic chip using nanoliter-size droplets, J. Am. Chem. Soc. 125 (2003) 11170–11171.
[5] X. Chen, H. Wu, C. Mao, G.M. Whitesides, A prototype two-dimensional capillary electrophoresis system fabricated in poly(dimethylsiloxane), Anal. Chem. 74 (2002) 1772–1778.
[6] S. Sugiura, M. Nakajima, S. Iwamoto, S. Seki, Interfacial tension driven monodispersed droplet formation from microfabricated channel array, Langmuir 17 (2001) 5562–5566.
[7] D.R. Link, S.L. Anna, D.A. Weitz, H.A. Stone, Geometrically mediated breakup of drops in microfluidic devices, Phys. Rev. Lett. 92 (2004) 054503/1–54503/4.
[8] Y.C. Tan, J. Fisher, A.L. Lee, V. Cristini, A.P. Lee, Design of microfluidic channel geometries for the control of droplet volume, chemical concentration, and sorting, Lab on a Chip 4 (2004) 292–298.
[9] T. Kawakatsu, Y. Kikuchi, M. Nakajima, Regular-sized cell creation in microchannel emulsification by visual microprocessing method, J. Am. Oil Chem. Soc. 74 (1997) 317–321.
[10] S.L. Anna, N. Bontoux, H.A. Stone, Formation of dispersions using "flow focusing" in microchannels, Appl. Phys. Lett. 82 (2003) 364–366.
[11] Q. Xu, M. Nakajima, The generation of highly monodisperse droplets through the breakup of hydrodynamically focused microthread in a microfluidic device, Appl. Phys. Lett. 85 (2004) 3726–3728.
[12] P. Garstecki, H.A. Stone, G.M. Whitesides, Mechanism for flow-rate controlled breakup in confined geometries: a route to monodisperse emulsions, Phys. Rev. Lett. 94 (2005) 164501.
[13] T. Thorsen, R. Roberts, F. Arnold, S. Quake, Dynamic pattern formation in a vesicle-generating microfluidic device, Phys. Rev. Lett. 86 (2001) 4163–4166.
[14] R. Dreyfus, P. Tabeling, H. Willaime, Ordered and disordered patterns in two-phase flows in microchannels, Phys. Rev. Lett. 90 (2003) 144505/1–144505/4.
[15] T. Nisisako, T. Torii, T. Higuchi, Droplet formation in a microchannel network presented at the international symposium on microchemistry and microsystems (ISMM 2001), Lab on a Chip 2 (2002) 24–26.
[16] T. Ward, M. Faivre, M. Abkarian, H.A. Stone, Microfluidic flow focusing: drop size and scaling in pressure versus flow-rate-driven pumping, Electrophoresis 26 (2005) 3716–3724.
[17] J.D. Tice, A.D. Lyon, R.F. Ismagilov, Effects of viscosity on droplet formation and mixing in microfluidic channels, Anal. Chim. Acta 507 (2004) 73–77.
[18] I. Kobayashi, M. Nakajima, K. Chun, Y. Kikuchi, H. Fujita, Silicon array of elongated through-holes for monodisperse emulsion droplets, AIChE J. 48 (2002) 1639–1644.
[19] I. Kobayashi, S. Mukataka, M. Nakajima, CFD simulation and analysis of emulsion droplet formation from straight-through microchannels, Langmuir 20 (2004) 9868–9877.
[20] J.H. Xu, G.S. Luo, G.G. Chen, J.D. Wang, Experimental and theoretical approaches on droplet formation from a micrometer screen hole, J. Membr. Sci. 266 (2005) 121–131.
[21] J.H. Xu, G.S. Luo, S.W. Li, G.G. Chen, Shear force induced monodisperse droplet formation in a microfluidic device by controlling wetting propert, Lab on a Chip 6 (2006) 131–136.
[22] J.H. Xu, S.W. Li, J. Tan, Y.J. Wang, G.S. Luo, Controllable preparation of monodisperse O/W and W/O emulsions in the same microfluidic device, Langmuir 22 (2006) 7943–7946.
[23] T. Mahidhar, X. Zhong, C. Ho, Bubble dispenser in microfluidic devices, Phys. Rev. E: Stat. Nonlinear Soft Matter Phys. 72 (2005) 037302.
[24] V. Cristini, Y.C. Tan, Theory and numerical simulation of droplet dynamics in complex flows—a review, Lab on a Chip 4 (2004) 257–264.
[25] H.A. Stone, A.D. Stroock, A. Ajdari, Engineering flows in small devices: microfluidics toward a lab-on-a-chip, Annu. Rev. Fluid Mech. 36 (2004) 388–411.